JOURNAL OF GUIDANCE, CONTROL, AND DYNAMICS
Vol. 18, No. 1, January–February 1995

New Formulation for General Spatial Motion of Flexible Beams

W. J. Haering*
General Motors Corporation, Warren, Michigan 48090-9055
R. R. Ryan†
Mechanical Dynamics, Inc., Ann Arbor, Michigan 48105
and
R. A. Scott‡
University of Michigan, Ann Arbor, Michigan 48109

A previously developed flexible body dynamic formulation for beam structures undergoing large overall prescribed planar motion is extended to the study of general spatial motion. The formulation, called the augmented imbedded geometric constraint (AIGC) approach, is restricted to small elastic deformations of the beam structure. The extension allows the study of a broader spectrum of problems involving systems with applied forces/torques where the overall motion is not known. Thus, the formulation can be used to study the two-way interaction between overall motion and local deformation that is fundamental to a general-purpose flexible body dynamic formulation. The AIGC approach describes the behavior with a set of differential equations linearized in terms of the deformation degrees of freedom (but not in the degrees of freedom describing the overall motion) and a number of constraint equations describing the physical attachments of the ends of beam. The effects of torsion, rotatory inertia, and an offset between the centroid and shear center of the beam (eccentricity) are included, but transverse shear deformation is neglected. The accuracy of the extended formulation is illustrated by comparing solutions of two problems to independently obtained solutions.

Introduction

INTEREST in flexible body dynamics, the coupling between large overall motion and local deformation in structural dynamics, has increased significantly since the early 1960s. Efforts to develop general-purpose analysis tools to address flexible body dynamics can be broken into two general classifications, nonlinear finite element approaches and rigid body dynamic approaches modified to allow local flexibility. The former strategy is used by Simo and Vu Quoc[1] and Christensen and Lee,[2] whereas the later is the approach adopted by Kane et al.[3] In Ref. 3, the authors discussed the need to develop element-specific approaches in order to include interrelationships between the components of local deformation. They developed a beam-specific formulation, often referred to as the imbedded geometric constraint (IGC) approach. A similar formulation was developed by Yoo,[4] referred to as the nonlinear strain displacement (NSD) approach, to overcome the inability of the IGC approach to accurately solve problems where the lateral deformation of the beam structure is dominated by membrane stiffness. However, the NSD approach does not reliably solve problems where the lateral deformation of the beam structure is dominated by bending stiffness. The inability of these two approaches to accurately solve both classes of problems prompted the authors[5] to develop another formulation that is capable of accurately solving both classes of problems. This new formulation is referred to as the augmented imbedded geometric constraint (AIGC) approach (restricted to planar prescribed motion in Ref. 5).

Here the AIGC approach is extended to general beam dynamics problems, with the assumption of small elastic local deformation. This is accomplished by permitting three-dimensional motion and deformation and allowing the overall motion to be unknown. The removal of the prescribed motion restriction allows the AIGC approach to study the two-way interaction between overall motion and local deformation, which is a fundamental issue in flexible body dynamics. As in Ref. 5, the development presented here involves the dynamics of a single beam. The extension of the AIGC approach presented in this paper closely follows the original IGC development in Ref. 3 and a subsequent extension[6] of that work to nonprescribed motion. As a result, this paper will concentrate on the major differences between the two approaches and will leave out many of the details covered in Refs. 3 and 6. Interested readers can also find a detailed presentation in the Ph.D. Dissertation of Haering.[7]

As discussed in Ref. 5, the primary difference between the AIGC and IGC approaches is that the differential equations of motion from the IGC approach, referred to as the system differential equations in the AIGC approach, have constraint equations added to enforce the physical boundary conditions for the beam structure. This set of differential equations with algebraic constraints forms the equations of motion for the AIGC approach. In addition, a set of general modal functions is employed in the AIGC approach to ensure the ability to satisfy any boundary conditions and to prevent inadvertently imposing boundary conditions that may not be correct for a specific problem.

Physical Model and System Differential Equations

The three-dimensional beam model is shown in Fig. 1. A flexible beam B is attached to a rigid base A at point O. The mass of body A is given by m_A, and the center of mass is located at a point A^* (not shown in Fig. 1). A dextral set of unit vectors, $\boldsymbol{a}_1, \boldsymbol{a}_2, \boldsymbol{a}_3$, is fixed in A, with the $\boldsymbol{a}_1$ direction aligned with the undeformed elastic axis of the straight beam. Following Kane et al.,[3] $\boldsymbol{a}_2$ and $\boldsymbol{a}_3$ are aligned with the principal area moment of inertia axes of the beam. Prior to deformation, a point on the elastic axis contained within a generic cross section, dB, is located at point C_0 at a distance x measured along the undeformed elastic axis. After deformation, that point on the elastic axis within cross section dB is located at point C, at a distance of $x + s$ measured along the deformed elastic axis. An additional set of dextral unit vectors, $\boldsymbol{b}_1, \boldsymbol{b}_2, \boldsymbol{b}_3$, are fixed in cross section dB and are aligned with $\boldsymbol{a}_1, \boldsymbol{a}_2, \boldsymbol{a}_3$, respectively, when the beam is undeformed. The mass per unit length of the

Presented as Paper 93-1435 at the 34th AIAA/ASME/ASCE/AHS/ASC Structures, Structural Dynamics, and Materials Conference, La Jolla, CA, April 19–21, 1993; received Jan. 28, 1993; revision received March 25, 1994; accepted for publication April 10, 1994.

*Senior Research Engineer, GM Research and Development Center. Member AIAA.
†Executive Vice President and Chief Operating Officer. Member AIAA.
‡Professor, Department of Mechanical Engineering and Applied Mechanics.

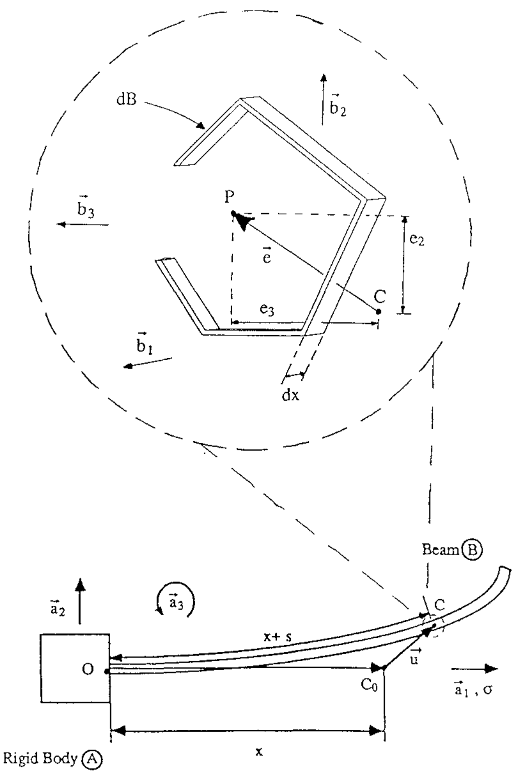

Fig. 1 Three-dimensional beam model.

beam is ρ, and the mass moments and products of inertia of A are J_{ij} $(i, j = 1, 2, 3)$, where i and j refer to the $\boldsymbol{a}_1, \boldsymbol{a}_2, \boldsymbol{a}_3$ unit vectors. The centroid of section dB is located at point P, which is offset from the point C on the elastic axis by the eccentricity vector $\boldsymbol{e}$ given by

$$\boldsymbol{e} = e_2\boldsymbol{b}_2 + e_3\boldsymbol{b}_3 \tag{1}$$

Allowing general three-dimensional deformation, the position vector from the attachment point O to the centroid P of dB is given by

$$\boldsymbol{p}^{\overline{OP}} = (x + u_1)\boldsymbol{a}_1 + u_2\boldsymbol{a}_2 + u_3\boldsymbol{a}_3 + e_2\boldsymbol{b}_2 + e_3\boldsymbol{b}_3 \tag{2}$$

where $u_1\boldsymbol{a}_1$, $u_2\boldsymbol{a}_2$, and $u_3\boldsymbol{a}_3$ represent orthogonal components of the beam deformation.

The orientation of section dB relative to body A can be described by three successive rotations of amounts θ_1, θ_2, and θ_3 about lines parallel to unit vectors $\boldsymbol{a}_1$, $\boldsymbol{a}_2$, and $\boldsymbol{a}_3$, respectively. This particular set of orientation angles is chosen to facilitate the introduction of beam torsion and rotatory inertia. The relative orientation of dB and A is described by the following direction cosine matrix:

$$^{A}C^{dB} = \begin{bmatrix} c_2c_3 & s_1s_2c_3 - s_3c_1 & c_1s_2c_3 + s_3s_1 \\ c_2s_3 & s_1s_2s_3 + c_3c_1 & c_1s_2s_3 - c_3s_1 \\ -s_2 & s_1c_2 & c_1c_2 \end{bmatrix} \tag{3}$$

where

$$^{A}C^{dB}_{ij} \equiv \boldsymbol{a}_i \cdot \boldsymbol{b}_j \qquad (i, j = 1, 2, 3) \tag{4}$$

and

$$s_i \equiv \sin\theta_i, \qquad c_i \equiv \cos\theta_i, \qquad i = 1, 2, 3 \tag{5}$$

Here θ_1 is introduced to account for twist and θ_2 and θ_3 allow shear deformation to be introduced (see Refs. 3 or 7).

Shear deformation is generally negligible in long beams, and it will not be included in this development. With it neglected, the angles θ_2 and θ_3 can be related to the spatial derivatives of the deformations u_2 and u_3 as

$$\theta_2 = -\frac{\partial u_3}{\partial x}, \qquad \theta_3 = \frac{\partial u_2}{\partial x} \tag{6}$$

The relations in Eq. (6) are then used to replace θ_2, θ_3, and all functions of those two variables, with functions of u_2 and u_3.

The deformation measures s, u_2, u_3, and θ_1 are represented as follows:

$$s = \sum_{j=1}^{\nu} \phi_{1j}(x)q_j(t), \qquad u_2 = \sum_{j=1}^{\nu} \phi_{2j}(x)q_j(t) \tag{7}$$

$$u_3 = \sum_{j=1}^{\nu} \phi_{3j}(x)q_j(t), \qquad \theta_1 = \sum_{j=1}^{\nu} \phi_{4j}(x)q_j(t) \tag{8}$$

where $\phi_{ij}(x)(i = 1, \ldots, 4, j = 1, \ldots, \nu)$ are modal functions the selection of which will be discussed later. The $q_j (j = 1, 2, \ldots, \nu)$ are the first ν generalized coordinates.

The system differential equations are developed using Kane et al.'s[8] approach. The contribution to the generalized active force from internal forces acting in the beam can be obtained from the following strain energy function V, which takes into account axial stretching, transverse bending, and torsion:

$$V = \frac{1}{2}\left[\int_0^L EA_0\left(\frac{\partial s}{\partial x}\right)^2 dx + \int_0^L G\kappa'\left(\frac{\partial \theta_1}{\partial x}\right)^2 dx + \int_0^L EI_2\left(\frac{\partial^2 u_3}{\partial x^2}\right)^2 dx + \int_0^L EI_3\left(\frac{\partial^2 u_2}{\partial x^2}\right)^2 dx\right] \tag{9}$$

where E, A_0, G, κ', I_2, and I_3 are the modulus of elasticity, cross-sectional area, shear modulus, effective torsional constant, and the area moments of inertia about the $\boldsymbol{b}_2$ and $\boldsymbol{b}_3$ axes, respectively.

Four measures of the beam deformation have been introduced s, u_1, u_2, and u_3, but due to the nature of beam deformation, only three are independent. They are related by the following relationship (see Refs. 4 or 7):

$$x + s = \int_0^x \left[\left(1 + \frac{\partial u_1}{\partial \sigma}\right)^2 + \left(\frac{\partial u_2}{\partial \sigma}\right)^2 + \left(\frac{\partial u_3}{\partial \sigma}\right)^2\right]^{1/2} d\sigma \tag{10}$$

where σ is a dummy variable of integration. This relationship can be reduced to the following more useful form (see Ref. 7):

$$u_1 = \sum_{j=1}^{\nu}\phi_{1j}q_j - \frac{1}{2}\sum_{j=1}^{\nu}\sum_{k=1}^{\nu}\left(\beta_{22}^x\right)_{jk}q_jq_k - \frac{1}{2}\sum_{j=1}^{\nu}\sum_{k=1}^{\nu}\left(\beta_{33}^x\right)_{jk}q_jq_k \tag{11}$$

where $(\beta_{km}^x)_{ij}$ is defined as

$$\left(\beta_{km}^x\right)_{ij} = \int_0^x \phi'(\sigma)_{ki}\phi'(\sigma)_{mj}d\sigma, \qquad i, j = 1, 2, \ldots, \nu, \qquad k, m = 2, 3 \tag{12}$$

where a prime in this case denotes a derivative with respect to σ. Note that $(\beta_{km}^x)_{ij}(i, j = 1, 2, \ldots, \nu, k, m = 2, 3)$ are indefinite integrals. For the shape functions chosen, they can be determined explicitly (see Ref. 7).

In this paper, only external forces applied to body A will be considered. Reference 6 contains a development including external forces applied to the beam structure itself and gravitational forces, and that development is directly applicable to the AIGC approach.

Forces and torques applied to body A can be replaced by an equivalent set, including a force acting through the mass center, $(\boldsymbol{R})^{A^*}$, and a torque $(\boldsymbol{T})^A$ as follows:

$$(\boldsymbol{R})^{A^*} = R_{1A}\boldsymbol{a}_1 + R_{2A}\boldsymbol{a}_2 + R_{3A}\boldsymbol{a}_3 \tag{13}$$

$$(\boldsymbol{T})^A = T_{1A}\boldsymbol{a}_1 + T_{2A}\boldsymbol{a}_2 + T_{3A}\boldsymbol{a}_3 \tag{14}$$

The discussion above highlights the essential mechanical ingredients of the theory. The derivation of the system differential equations is quite lengthy, and details will not be given here. They can be found in Refs. 3 and 6 (transverse shear deformation included) and also in Ref. 7 (both with and without transverse shear deformation included).

The system differential equations for nonprescribed motion are given by the form

$$\sum_{j=1}^{\nu+6} \hat{M}_{ij}\dot{u}_j^* + \sum_{j=1}^{\nu+6} \hat{G}_{ij}u_j^* + \sum_{j=1}^{\nu+6} \hat{K}_{ij}q_j = \hat{F}_i, \qquad i = 1, 2, \ldots, \nu+6 \tag{15}$$

The first ν generalized coordinates $(q_j, j = 1, 2, \ldots, \nu)$ were introduced above. The last six generalized coordinates $(q_j, j = \nu+1, \ldots, \nu+6)$ are angular, and translational measures used to describe the orientation and location of the rigid base, body A, in the Newtonian reference frame. The first ν generalized speeds $(u_j^*, j = 1, 2, \ldots, \nu)$ are the time derivatives of the corresponding generalized coordinates. The remaining six generalized speeds $(u_j^*, j = \nu+1, \ldots, \nu+6)$ describe the overall motion of the body A. The $\nu+6$ unknowns $(\dot{u}_j^*, j = 1, 2, \ldots, \nu+6)$ are the time derivatives of the generalized speeds. The matrices $\hat{M}$, $\hat{G}$, and $\hat{K}$ contain, in addition to constants (resulting from integrals over the domain of the beam), terms involving the generalized coordinates and/or generalized speeds. The column matrix $\hat{F}$ contains nonlinear terms in the generalized coordinates and generalized speeds. It should be noted that, because of the nature of matrices $\hat{M}$, $\hat{G}$, $\hat{K}$, and $\hat{F}$, the set of differential equations in Eq. (15) is nonlinear.

Constraint Equations and Modal Function Selection

The use of constraint equations to enforce the beam boundary conditions and proper selection of the corresponding global shape (modal) functions are the primary differences between the AIGC approach and the IGC and NSD approaches (Refs. 3, 4, and 6). As demonstrated in Ref. 5, the use of constraints and proper modal function selection allows the AIGC approach to accurately solve beam dynamics problems where the lateral deformations of the beam are dominated by either bending or membrane stiffness. This stems from the ability of the AIGC approach to enforce boundary conditions that cannot be explicitly defined in the deformation measures chosen.

In particular, the previously developed IGC approach uses s, u_2, and u_3 as deformation measures and can only ensure satisfaction of boundary conditions explicitly defined in those deformation measures. As a result, the IGC approach fails to accurately solve beam problems where the lateral deformations are dominated by membrane stiffness, which includes a boundary condition explicitly described in terms of the u_1 deformation measure. Conversely, the NSD approach uses the u_1, u_2, and u_3 deformation measures and therefore can only ensure satisfaction of boundary conditions explicitly defined in those deformation measures. Thus, the NSD approach fails to accurately solve some beam problems where the lateral deformations are dominated by bending stiffness, which includes boundary conditions explicitly described in terms of the s deformation measure. The AIGC approach overcomes these limitations by enforcing boundary conditions that are not explicitly defined in terms of the chosen deformation measures through the use of constraint equations. Furthermore, the general nature of the AIGC approach allows the solution of problems where the dominant elastic effects are not known a priori.

The physical boundary conditions for the beam can be related to the deformations at the beam ends. This is accomplished directly with the relationships in Eqs. (7), (8), and (11) for deformation conditions or with spatial derivatives of those relationships for force or moment conditions.

Specifically, consider a beam cantilevered to a rigid mass, as the one shown in Fig. 1. The boundary conditions for that beam are those for a cantilever beam with the built-in end located at $x = 0$ and the free end at $x = L$ and are given by the following:

$$\begin{aligned}
&s|_{x=0} = 0, && u_2|_{x=0} = 0,\\
&u_3|_{x=0} = 0, && \theta_1|_{x=0} = 0\\
&\left.\frac{\partial u_2}{\partial x}\right|_{x=0} = 0, && \left.\frac{\partial u_3}{\partial x}\right|_{x=0} = 0,\\
&\left.\frac{\partial s}{\partial x}\right|_{x=L} = 0, && \left.\frac{\partial^3 u_2}{\partial x^3}\right|_{x=L} = 0\\
&\left.\frac{\partial^3 u_3}{\partial x^3}\right|_{x=L} = 0, && \left.\frac{\partial \theta_1}{\partial x}\right|_{x=L} = 0,\\
&\left.\frac{\partial^2 u_2}{\partial x^2}\right|_{x=L} = 0, && \left.\frac{\partial^2 u_3}{\partial x^2}\right|_{x=L} = 0
\end{aligned} \tag{16}$$

Corresponding to these 12 boundary conditions are 12 constraint equations relating the deformation generalized coordinates $q_j(t)(j = 1, \ldots, \nu)$:

$$\begin{aligned}
&\sum_{j=1}^{\nu} \phi_{kj}(0)q_j = 0, && k = 1, 2, 3, 4\\
&\sum_{j=1}^{\nu} \phi'_{kj}(0)q_j = 0, && k = 2, 3\\
&\sum_{j=1}^{\nu} \phi'_{kj}(L)q_j = 0, && k = 1, 4\\
&\sum_{j=1}^{\nu} \phi''_{kj}(L)q_j = 0, && k = 2, 3\\
&\sum_{j=1}^{\nu} \phi'''_{kj}(L)q_j = 0, && k = 2, 3
\end{aligned} \tag{17}$$

where a prime in this case denotes a derivative with respect to x. For simplicity, the 12 constraints expressed in Eq. (17) are represented as

$$\Theta_k = 0, \qquad k = 1, 2, \ldots, 12 \tag{18}$$

The modal functions $\phi_{ij}(x)(i = 1, \ldots, 4, j = 1, \ldots, \nu)$ are developed using the substructuring techniques developed by Craig and Bampton[9] and are discussed in depth in Refs. 5 and 7. This technique subdivides the modal functions into two subsets called dynamic and static modal functions. For the sake of completeness, that procedure will be briefly discussed here.

The same modal functions are used to describe the lateral deformation measures u_2 and u_3. On the other hand, the axial stretch s and the twisting deformation θ_1 are described by a different single set of modal functions. The same modal functions are used for the axial stretch and twist, because, for a simple rod, axial and twisting behavior is governed by wave equations of the same basic form.

The lateral dynamic modal functions are developed from an eigenanalysis for lateral vibration of a nonrotating beam with boundary conditions of zero displacement and zero slope at both ends. The lateral static modes are obtained by applying unit displacements (or rotations) in the directions held fixed in developing the dynamic modes. While enforcing each unit displacement or rotation, the other displacements or rotations are held fixed. For example, one such shape function satisfies the conditions $\phi(0) = 1$ and $\phi'(0) = \phi(L) = \phi'(L) = 0$, where ϕ is a generic static shape function.

For the stretch/twist modal functions, the dynamic functions are developed from an eigenanalysis for axial vibration of a nonrotating rod with boundary conditions of zero displacement at both ends. The static modes are obtained by applying unit displacements at each end while holding the other end fixed.

This method of selecting the modal functions serves two purposes. First, the set of modal functions are general enough to satisfy any boundary condition. Second, they do not satisfy any particular end condition; thus they prevent inadvertently satisfying any boundary condition that may be incorrect for the problem at hand.

Equations of Motion and Solution Technique

The final equations of motion are obtained by combining the system differential equations [Eq. (15)] with the constraint equations describing the appropriate boundary conditions [Eq. (18) for the bending stiffness dominated problem being considered] to form a set of differential-algebraic equations. Thus, for the case being considered (nonprescribed motion and bending dominated lateral deformations), the equations of motion are

$$\sum_{j=1}^{\nu+6} \hat{M}_{ij}\dot{u}_j^* + \sum_{j=1}^{\nu+6} \hat{G}_{ij}u_j^* + \sum_{j=1}^{\nu+6} \hat{K}_{ij}q_j = \hat{F}_i,$$

$$i = 1, 2, \ldots, \nu + 6 \qquad \Theta_k = 0, \qquad k = 1, 2, \ldots, 12 \tag{19}$$

In the case where the overall motion is assumed known, there are six fewer differential equations than there are in Eq. (19) (see Ref. 7). It is worth noting that the system differential equations are linear (but with time-varying coefficients) when the motion is known.

For the results about to be discussed, the equations of motion were solved using Baumgarte's[10] approach. In general, the values of the constraint stabilization parameters α and β are chosen such that no significant constraint drift is noticed over the range of simulation. In the results provided subsequently, the values $\alpha = \beta = 0$ were found to be satisfactory (nonzero values for α and β were required for work presented in Ref. 5).

Verification

The validity of this spatial extension of the AIGC approach will be investigated by comparing simulations for two distinct problems. First, a nonprescribed motion problem will be investigated, demonstrating the ability of the AIGC approach to capture the two-way coupling between overall motion and local deformation associated with this type of problem. Second, a three-dimensional prescribed motion problem for a beam with an offset of the shear center and centroid, commonly referred to as noncompact, will be investigated. This problem exhibits multiaxial coupling not present in the two-dimensional work in Ref. 5 and coupling introduced by the offset of the shear center and centroid.

The ability to accurately describe nonprescribed motion problems is demonstrated by analyzing a problem studied by Ryan[6], namely a torque prescribed about the $\boldsymbol{a}_3$ axis for the system shown in Fig. 1. The mass and inertia properties of the rigid base and the characteristics of the beam are given in Table 1. In addition, the beam is attached to body A at a point offset from the mass center by the vector $1\boldsymbol{a}_1 + 0\boldsymbol{a}_2 + 0\boldsymbol{a}_3$ (measured in meters). The applied torque [(defined in Eq. (14)] is given by

$$T_{3A} = \begin{cases} 0.1\,\text{N-m}, & \text{if} \quad 0 < t \le 5\,\text{s} \\ 0\,\text{N-m}, & \text{if} \quad t > 5\,\text{s} \end{cases} \tag{20}$$

The $\boldsymbol{a}_3$ measure of the angular velocity is shown in Figs. 2 (AIGC) and 3 (Ryan's IGC solution). It is seen that the results are almost identical. Similar results were also found for the beam deformation but are not given here. This simulation demonstrates the ability of the AIGC approach to accurately solve simultaneously for overall motion and local deformation when forces/torque are applied.

The three-dimensional prescribed motion problem is illustrated in Fig. 4. Links L_1 and L_2 are assumed rigid (length of 8 m); link L_3, possessing a channel section, is analyzed as a flexible beam (see Table 2 for characterization) with the AIGC approach. The motion (angles of rotation) of the joints is described by the following (where $T = 15$ s):

$$\psi_1(t) = \begin{cases} \pi - \dfrac{\pi}{2T}\left(t - \dfrac{T}{2\pi}\sin\dfrac{2\pi t}{T}\right)\text{rad} & \text{if} \quad 0 \le t \le T \\ \dfrac{\pi}{2}\,\text{rad} & \text{if} \quad t > T \end{cases} \tag{21}$$

$$\psi_2(t) = \begin{cases} \pi - \dfrac{3\pi}{4T}\left(t - \dfrac{T}{2\pi}\sin\dfrac{2\pi t}{T}\right)\text{rad} & \text{if} \quad 0 \le t \le T \\ \dfrac{\pi}{4}\,\text{rad} & \text{if} \quad t > T \end{cases} \tag{22}$$

$$\psi_3(t) = \begin{cases} \pi - \dfrac{\pi}{T}\left(t - \dfrac{T}{2\pi}\sin\dfrac{2\pi t}{T}\right)\text{rad} & \text{if} \quad 0 \le t \le T \\ 0\,\text{rad} & \text{if} \quad t > T \end{cases} \tag{23}$$

This problem, similar to one studied by Kane et al.,[3] was simulated using the AIGC approach and a discrete ADAMS[11] model. The results for the lateral, axial, and twisting deformations of the beam tip are given in Figs. 5–8. Excellent agreement as regards u_3 is seen in Fig. 5. Also, excellent agreement for u_2 during the forced-response portion is seen in Fig. 6. Differences in phase and amplitudes are seen in the free-response portion. Some significant differences as regards the predictions of the axial and twist deflection are noted from Figs. 7 and 8. Definitive conclusions relative to the accuracy of these deformations cannot be made without additional independent solutions.

Table 1 Physical constants for spatial nonprescribed motion problem

$L = 20$ m	$m_A = 120$ kg
$\rho = 0.2$ kg/m	$J_{11} = 100$ kg-m^2
$E = 1.0 \times 10^{10}$ N/m^2	$J_{22} = 50$ kg-m^2
$G = 5 \times 10^9$ N/m^2	$J_{33} = 130$ kg-m^2
$A_0 = 9.30 \times 10^{-2}$ m^2	$J_{12} = J_{13} = J_{23} = 0$
$I_2 = I_3 = 5 \times 10^{-10}$ m^4	$e_2 = e_3 = 0$
$\kappa' = 1.2 \times 10^{-9}$ m^4	

Table 2 Flexible-beam characterization for spatial prescribed motion problem

$L_3 = 8$ m	$I_2 = 4.8746 \times 10^{-9}$ m^4
$\rho = 2.02$ kg/m	$I_3 = 8.2181 \times 10^{-9}$ m^4
$E = 1.0 \times 10^{10}$ N/m^2	$\kappa' = 2.446 \times 10^{-11}$ m^4
$G = 5 \times 10^9$ N/m^2	$e_2 = 0$
$A_0 = 7.3 \times 10^{-5}$ m^2	$e_3 = 0.0185$ m

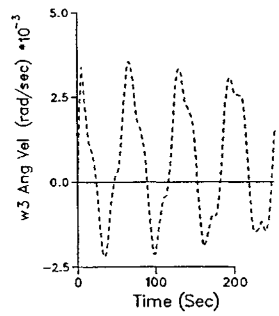

Fig. 2 Overall beam angular velocity (AIGC) for spatial nonprescribed motion problem.

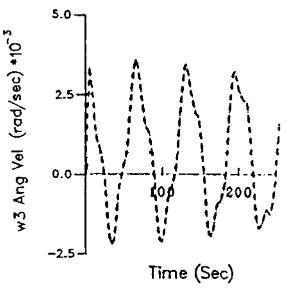

Fig. 3 Overall beam angular velocity (Ryan) for spatial nonprescribed motion problem.

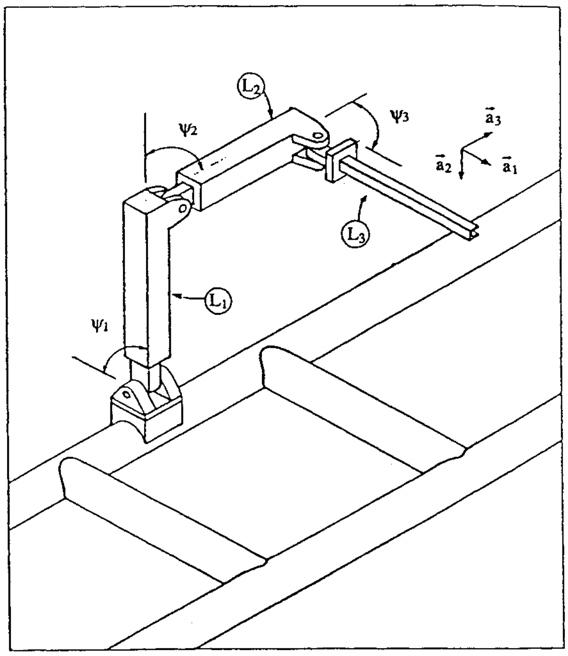

Fig. 4 Physical system for spatial prescribed motion problem.

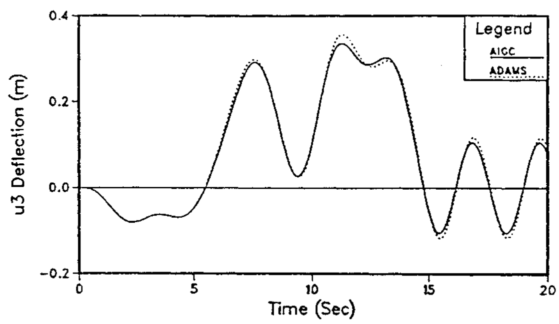

Fig. 5 Lateral (u_3) beam tip deflection for spatial prescribed motion problem.

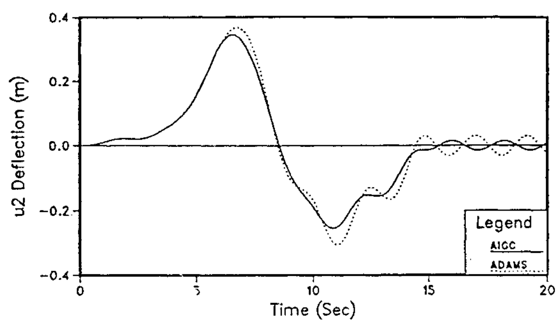

Fig. 6 Lateral (u_2) beam tip deflection for spatial prescribed motion problem.

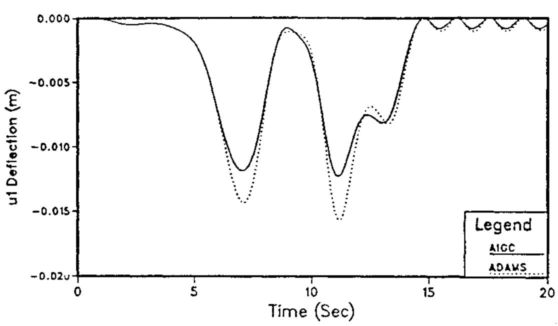

Fig. 7 Axial beam tip deflection for spatial prescribed motion problem.

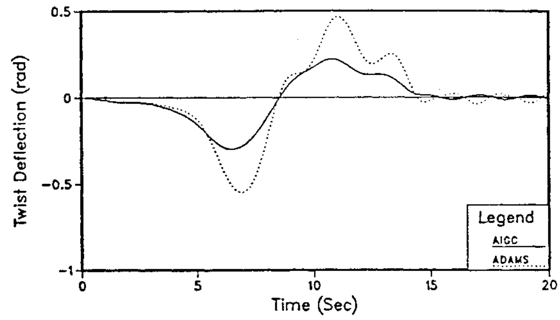

Fig. 8 Axial beam tip twist deflection for spatial prescribed motion problem.

Additional Classes of Problems

All problems that have been addressed in this paper and in Ref. 5 have beam boundary conditions that are time invariant and are explicitly zero. The AIGC approach could be easily adapted to problems where the above restriction does not apply. For example, consider adding a rigid mass at the free end of the beam shown in Fig. 1; in this case, the bending moment, transverse shear load, and axial strain are not zero at the right-hand end but are related to the acceleration and angular acceleration (time varying) of the attached mass. The mass at the right-hand end has to be treated differently from the one at the left (rigid base) because of the coordinate system employed. The AIGC approach could be extended to such problems by rewriting the constraints used to enforce the boundary conditions.

Conclusions

In this paper, the AIGC approach has been extended to allow three-dimensional motion and deformation, and the overall motion is no longer restricted to a known function of time. This extended capability has been demonstrated by investigating the following two problems: 1) a problem with an applied torque (nonprescribed motion), exhibiting two-way coupling between local deformation and overall motion, and 2) a three-dimensional prescribed motion problem with torsion and eccentricity. Excellent agreement with an existing solution was shown for the first problem. For the second problem, good agreement of the lateral deformation to an independent solution was shown. Differences for the axial and twist deformation as compared to that independent solution were found. The ultimate resolution of these differences awaits additional independent solutions.

References

[1]Simo, J. C., and Vu Quoc, L., "On the Dynamics of Flexible Beams Under Large Overall Motions—The Plane Case: Parts I & II," *Journal of Applied Mechanics,* Vol. 53, No. 4, 1986, pp. 849–863.

[2]Christensen, E. R., and Lee, S. W., "Nonlinear Finite Element Modeling of the Dynamics of Unrestrained Flexible Structures," *Computers and Structures,* Vol. 23, No. 6, 1986, pp. 819–829.

[3]Kane, T. R., Ryan, R. R., and Banerjee, A. K., "Dynamics of a Cantilever Beam Attached to a Moving Base," *Journal of Guidance, Control, and Dynamics,* Vol. 10, No. 2, 1987, pp. 139–151.

[4]Yoo, H. H., "Dynamic Modeling of Flexible Bodies in Multibody Systems," Ph.D. Dissertation, University of Michigan, Ann Arbor, MI, 1989.

[5]Haering, W. J., Ryan, R. R., and Scott, R. A., "New Formulation for Flexible Beams Undergoing Large Overall Plane Motion," *Journal of Guidance, Control, and Dynamics,* Vol. 17, No. 1, 1994, pp. 76–83.

[6]Ryan, R. R., "Simulation of Actively-Controlled Flexible Spacecraft," *Journal of Guidance, Control, and Dynamics,* Vol. 13, No. 4, 1990, pp. 691–702.

[7]Haering, W. J., "A New Flexible Body Dynamic Formulation for Beam Structures Undergoing Large Overall Motion," Ph.D. Dissertation, Univ. of Michigan, Ann Arbor, MI, May 1992.

[8]Kane, T. R., and Levinson, D. A., *Dynamics, Theory and Applications,* McGraw-Hill, New York, 1983.

[9]Craig, R. R., and Bampton, M. C. C., "Coupling of Substructures for Dynamic Analysis," *AIAA Journal,* Vol. 6, No. 7, 1968, pp. 1313–1319.

[10]Baumgarte, J. W., "Stabilization of Constraints and Integrals of Motion in Dynamical Systems," *Computer Methods in Applied Mechanics and Engineering,* Vol. 1, No. 1, 1972, pp. 1–16.

[11]Anon., ADAMS 5.2 User's Manual, Mechanical Dynamics Inc., Ann Arbor, MI, April 1987.